ACS APPLIED MATERIALS & INTERFACES

Research Article

www.acsami.org

Steam-Etched Spherical Carbon/Sulfur Composite with High Sulfur Capacity and Long Cycle Life for Li/S Battery Application

Meiri Wang, Hongzhang Zhang,* Qian Wang, Chao Qu, Xianfeng Li, and Huamin Zhang*

Energy Storage Division, Dalian Institute of Chemical Physics, Chinese Academy of Sciences, Dalian 116023, China

ABSTRACT: Spherical carbon material with large pore volume and specific area was designed for lithium/sulfur (Li/S) soft package battery cathode with sulfur loading over 75%, exhibiting good capacity output (about 1300 mAh g^{-1}-S) and excellent capacity retention (70% after 600 cycles) at 0.1 C. The spherical carbon is prepared via in situ steam etching method, which has the advantages of low cost and easy scale up.

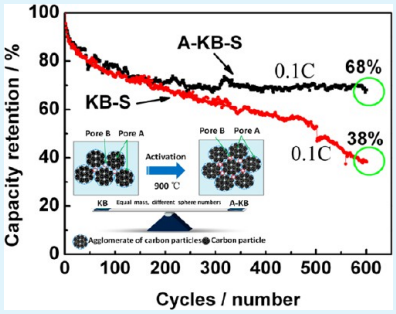

KEYWORDS: *spherical carbon material, large pore volume, lithium sulfur battery, carbon−sulfur composite, water−steam activation*

INTRODUCTION

With the increasing demand for efficient and economic energy storage devices, Li−S batteries become one of the most attractive candidates for the next generation of high-energy rechargeable battery because of their high theoretical specific capacity (1675 Ah kg^{-1}), high theoretical energy density (2600 Wh kg^{-1}), and economic cost.[1−4] However, the electrochemical properties of sulfur bring noticeable problems that hinder their practical application. First, sulfur and its various discharge products (Li_2S_x, x = 1−8) show poor ionic and electronic conductivity, which leads to poor active material utilization in the cathode. Second, the intermediate product Li_2S_x (mainly Li_2S_4−Li_2S_8) can be easily dissolved into the organic solvent of electrolyte, leading to irreversible capacity fade of the cathode and the so-called "shuttle effect" that further deteriorates the battery performances by forming the Li_2S_2 or Li_2S electrochemically inactive layer on the anode. Besides that, the volume difference between S and Li_2S could cause serious volume fluctuation (shrinkage and expansion), which further decrease the cycle stability of Li/S battery.

To overcome these problems, combining sulfur with carbon material is generally accepted as an effective solution. According to massive research work,[4−17] the ideal porous carbon is supposed to have good electronic conductivity, large electrochemical reaction interface (large surface area), proper porous structure for electrolyte infiltration (or Li^+ transportation), micro/mesoscale pore size, and large pore volume for trapping the polysulfide, together with low cost and eco-friendly manufacturing processes.

During the past 20 years, great efforts have been engaged in the carbon material development. Park et al.[18] designed a kind of porous carbon (surface area 699.76 m^2 g^{-1}) incorporated with sulfur, which maintained about 70% of its initial discharge capacity after 50 cycles test at 0.1 C (168 mA g^{-1}) between 1.8 and 2.6 V. Nazar's group[19] reported a unique nanoscale spherical ordered mesoporous carbon with extremely high bimodal pore volume (2.32 cm^3 g^{-1}) and large surface area (2445 m^2 g^{-1}) acquired via a two-step casting process, showing highly reversible capacity (1200 mAh g^{-1} S) and excellent cycling efficiency. Other researchers have also developed many kinds of porous carbon materials with advanced Li/S battery performance.[6,12,20−33]

Carbon materials with controlled morphology and tunable pore structure have shown excellent performance.[34−38] However, most reported results on Li−S batteries are obtained from cathodes with a low sulfur content of only about 60 wt %, which significantly reduces the overall energy density, although a very high specific capacity of sulfur was obtained.[25−27,39] According to Wang et al.,[40] this phenomenon is caused by the relatively insufficient pore volume inner the carbon materials. Our group also found that higher sulfur utilization and cycling stability could be achieved via increasing the mesoporous volume of carbon materials.[41] Furthermore, to avoid the structure collapse of the cathode, more free volume (about 80%) should better be reserved inside the carbon pores to fit the volume expanded from S_8 to Li_2S. However, the pore volume of most developed carbon materials is below 3.0 cm^3 g^{-1},[19] which should be further increased. Besides that, the carbon pores should better be micro or meso pores (<100 nm) for trapping the Li_2S_n via capillary suction force.[42] Currently, although several kinds of carbon materials with large mesopore volume and good battery performance have been successfully explored, their cost is usually too high for practical application due to the complicated multistep process.

In this study, a novel kind of spherical porous carbon with desired porous structure was developed through in situ etching

Received: October 30, 2014
Accepted: January 26, 2015
Published: January 26, 2015

DOI: 10.1021/am5075562
ACS Appl. Mater. Interfaces 2015, 7, 3590−3599

Scheme 1. Schematic Illustration of Different Pore Structures Inside the Agglomerate of Carbon Particles and the Electrochemical Processes for the Agglomerate Of KB-S and A-KB-S Carbon Particles[ab]

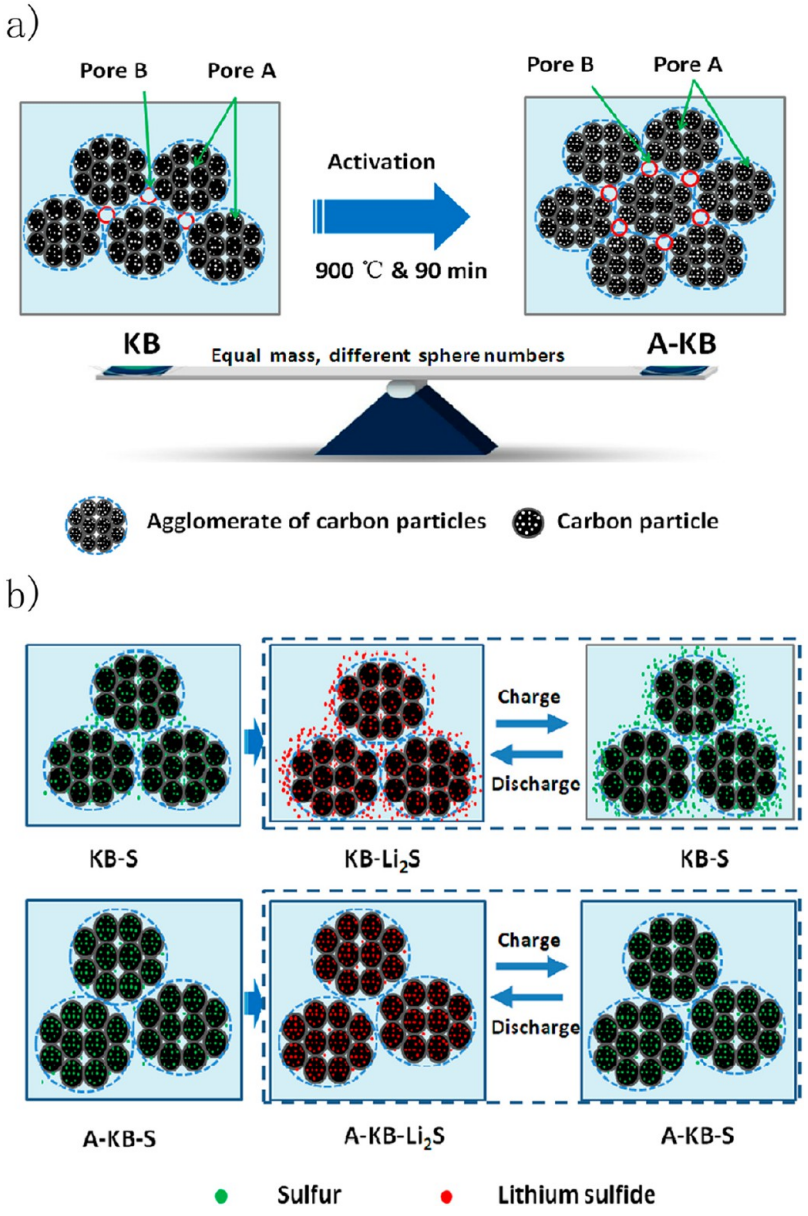

[a]The different pore structure inside the agglomerate of carbon particles: KB (before activation). The A-KB carbon has many more spheres compared to KB carbon of the same mass. The volumes of pore A (3−4 nm) and pore B (about 40 nm) in A-KB carbon are also larger than those in KB carbon. [b]The electrochemical processes for the agglomerate of KB-S and A-KB-S carbon particles (partial enlarged plots). The A-KB carbon particles have many more mesopores to hold sulfur than do pristine KB carbon particles. Compared to KB-S, the A-KB-S composite exhibits better reversible distribution of sulfur particles in the abundant pore volume.

the Kejent black (KB) carbon with water steam. The as-prepared carbon sphere (A-KB) achieved the largest mesopore volume (4.0 cm^3 g^{-1}) ever reported for Li/S application, together with high surface area (1510 m^2 g^{-1}) and appealing low cost. Compared with pristine KB carbon (Scheme 1), the as prepared A-KB carbon showed larger free volume to trap the sulfur and transport the Li^+ through the carbon pores, which could lead to more uniform sulfur reversible distribution, more unobstructed Li^+ transport channel, better capacity retention and structure stability. Also in this study, the in situ steam etching mechanism was studied carefully, and the structure−performance relationship between the carbon materials and Li/S batteries was analyzed in detail. This work would shed light on the development of Li/S batteries.

EXPERIMENTAL SECTION

Material Preparation. The in situ etching of the Kejent black (KB) nanoparticles was prepared as follows. First, 10 g of pristine KB nanoparticles were put in a quartzose vessel and dried at 120 °C for 5 h. Second, the Kejent black powder was put into the furnace and heated to 900 °C at 5 °C min^{-1} under argon atmosphere. Then, water steam was added into the furnace with the flux of 600 mL min^{-1} and kept for 90 min. Finally, the as-prepared spherical carbon particles (named A-KB) were obtained after cooling to room temperature in argon atmosphere.

DOI: 10.1021/am5075562
ACS Appl. Mater. Interfaces 2015, 7, 3590−3599

The sulfur−carbon (S−C) composite was prepared by incorporating the sublimed sulfur into the porous carbon via melt-diffusion method. Typically, the A-KB and sulfur were mixed with ball-milling for 6 h before heated to 155 °C for 15 h in argon filled vessel, named as A-KB-S. For comparison, the pristine KB and sulfur composite was also prepared by the same method as above, named as KB-S. For both samples, the sulfur content is 75 wt %.

Materials Characterizations. Brunauer−Emmett−Teller (BET) method was used for the surface area measurement. Barrett−Joyner−Halenda (BJH) adsorption−desorption was used for the pore analysis. Morphology of the A-KB and A-KB-S composite was characterized by scanning electron microscopy (SEM) on a QUANTA 200 FEG operated at 20 kV. To investigate the redistribution of the sulfur in the A-KB-S composite, we performed the sulfur element analysis on QUANTA 200 FEG operating at 20 kV, and the sulfur content was analyzed in Argon on a Pyris Diamond TGAA/DTA analyzer (PerkinElmer) at a heating rate of 5 °C min^{-1}. The state of pure sulfur after loading has been characterized by X-ray diffraction (XRD) operating at 40 kV and 40 mA (DX-2700). The oxygen on the surface of carbon was detected by X-ray photoelectronspectroscopy (XPS) which was carried out via a surface analysis system (ESCALAB250) equipped with monochromatic Al Kα radiation. The XPS spectra were peak fit and analyzed using XPSPeak4.1 (Photoelectron Spectroscopy Lab, Seoul National University).

Electrode Fabrications and Evaluations. The A-KB-S composite was mixed with acetylene black and poly(vinylidene fluoride) binder at a weight ratio of 80:10:10 in anhydrous *N*-methyl-2-pyrolidinone (NMP) to form a slurry, which was coated onto Al foil and dried at 65 °C under vacuum. The active material loading in the electrode is 1.0 mg cm^{-2}.

Soft-pouch cells (2.5 × 5 cm or 4.8 × 10 cm) were assembled in an argon-filled glovebox with lithium foil as the anode, Cellgard 2325 as the separator and 1.5 M LiTFSI in DME/DOL (1:1 by volume) as the electrolyte. (LiTFSI: Bis(trifluoromethane) sulfonimide lithium, Guotai-Huarong New Chemical Materials Corp; DME: dimethoxyethane, Guotai-Huarong New Chemical Materials Corp. and DOL: 1, 3-dioxolane, Guotai-Huarong New Chemical Materials Corp.). The charge−discharge test was carried out using LAND CT-2001A equipment (Wuhan Landian Corp.), and the cutoff voltage for charge and discharge was set to 2.8 and 1.5 V, respectively. The cycling voltammetry (CV) measurement was conducted using a CHI 611 electrochemical workstation (Shanghai Chenhua Corp.) at a scan rate of 0.1 mV s^{-1} from 1.5 to 3.0 V. Electrochemical impedance spectroscopy (EIS) measurement was conducted in a frequency range from 3.0 × 10^5 Hz to 100 mHz at open-circuit voltage (OCV) with the amplitude of 10 mV on a Solartron 1287 electrochemical workstation.

RESULTS AND DISCUSSIONS

The water steam etching mechanism of KB particles is illustrated in Scheme 2 and is based on previous literature.[23,43] First, water steam is absorbed into the pores of the carbon particles, and then it reacts with carbon under high temperature. During this process, more abundant micro- and mesopores are formed inside the carbon sphere after a series of carbon gasification reactions (Scheme 2) that release CO, CO_2, and H_2. Therefore, we speculate that the surface area and pore volume of the KB particles would increase while maintaining the morphology.

Scheme 2. Schematic Illustration of Water Steam Activation Process

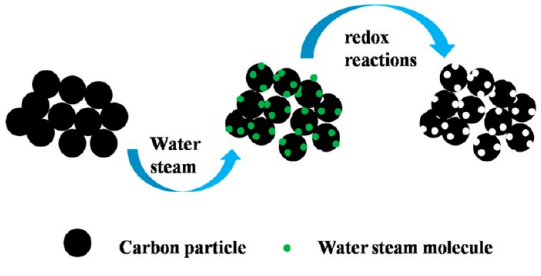

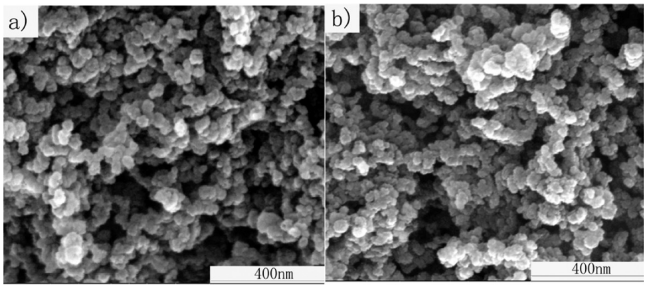

Figure 1. SEM images of (a) pristine surface morphologies of A-KB carbon particles and (b) pristine surface morphologies of KB carbon particles.

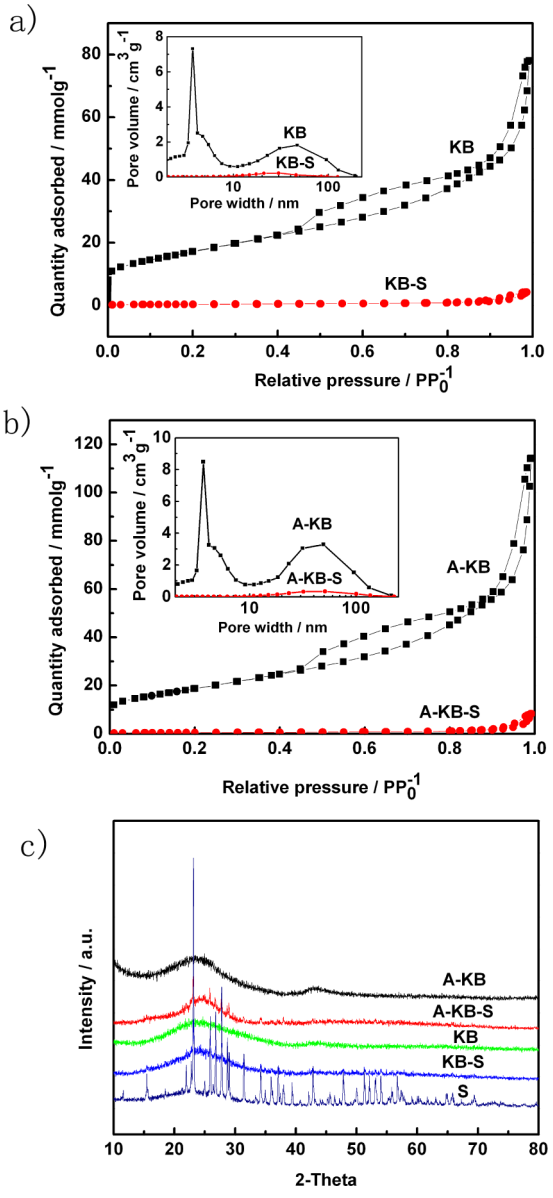

Figure 2. (a and b) Pore-size distribution curves of samples KB, KB-S, A-KB, and A-KB-S and (c) X-ray diffraction curves of S, KB, KB-S ,A-KB, and A-KB-S composites.

DOI: 10.1021/am5075562
ACS Appl. Mater. Interfaces 2015, 7, 3590−3599

Table 1. Pore Volume[a] and BET Surface Area for Carbons and Corresponding C–S Composites

parameters	samples			
	KB	KB-S	A-KB	A-KB-S
total surface area (m^2 g^{-1}-C)	1349	114.8	1511	140
total pore volume (cm^3 g^{-1}-C)	2.60	0.6	4.00	1.16
pore volume$_{10-100\ nm}$ (cm^3 g^{-1}-C)	1.59	0.56	2.53	1.12
pore volume$_{<10\ nm}$ (cm^3 g^{-1}-C)	1.15	0.04	1.54	0.04

[a]Pore volume calculated by BJH method from desorption curve.

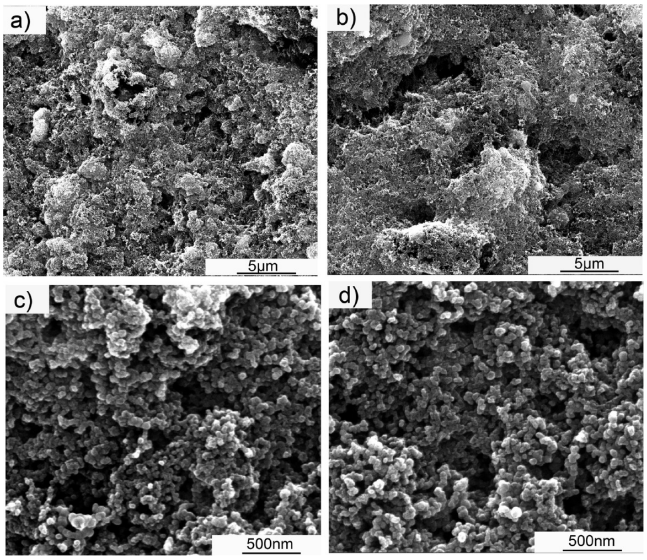

Figure 3. SEM images of pristine surface morphologies at different magnifications: (a and c) A-KB-S composite electrode and (b and d) KB-S composite electrode.

$$C + H_2O \rightarrow CO + H_2$$

$$CO + H_2O \rightarrow CO_2 + H_2$$

$$CO_2 + C \rightarrow 2CO$$

Our speculation was preliminarily proved by observing the carbon sphere morphology directly. As shown in Figure 1, the A-KB exhibits the similar spherical morphology with KB, confirming that water steaming etch process did not destroy the outer morphology of the carbon particles. However, the inner porous structure of the carbon sphere changed obviously. Quantitative pore parameters of both KB and A-KB before sulfur loading were derived from the BJH and BET methods. The degassed temperature for both KB and A-KB before and after sulfur loading was 350 and 50 °C respectively. As shown in Figure 2a,b, the pore sizes of both carbon samples are centered at 3–4 and 40 nm, defined as pore A and pore B, respectively. Both the KB and A-KB have comparable volumes of pore A (Table 1); however, the A-KB shows much larger volume of pore B. Therefore, A-KB exhibits higher BET surface area (1510 m^2 g^{-1}) than pristine KB (1349 m^2 g^{-1}). The results demonstrate that the water steam etching method mainly influenced the formation of pore B, which mainly induced the pore volume increasing from 2.6 cm^3 g^{-1} to 4.0 cm^3 g^{-1}.

However, the difference between KB-S and A-KB-S seems negligible after sulfur loading, with similar surface area and pore volume (Table 1). The phenomenon was caused by the

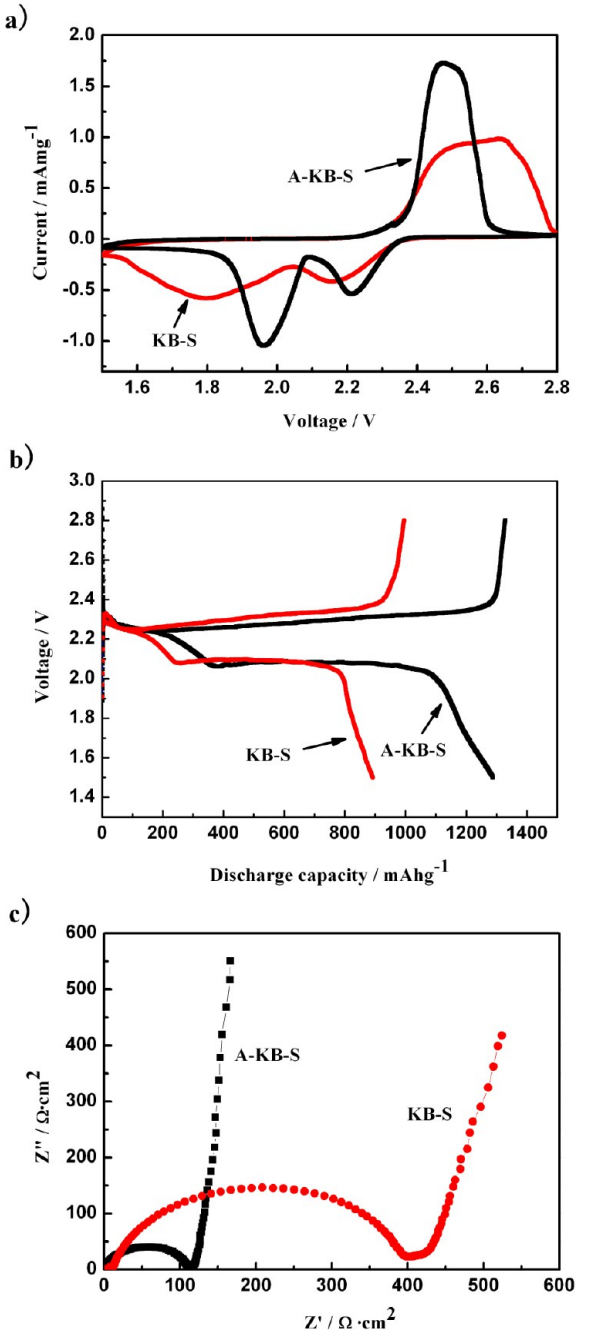

Figure 4. (a) CV curves of A-KB-S and KB-S composite electrodes at a scan range of 2.8–1.5 V and a scan rate of 0.1 mV s^{-1}. (b) Discharge/charge curves of A-KB-S and KB-S composite electrodes at 0.1 C. (c) Electrochemical impedance spectrum of A-KB-S and KB-S composite electrodes in Li–S batteries before initial discharge.

blockage of surface pores with sulfur particles, which might affect the detection of the inner pores in carbon spheres. In spite of this, all the inner pores could be utilized for Li_2S_n reaction and redistribution during cycling process, which is consistent with the XRD characterization in Figure 2c. Only very tiny characteristic XRD peaks of the pure S phase can be detected in A-KB-S and KB-S composites, indicating the uniform S distribution.[23]

The surface morphologies of A-KB-S and KB-S electrodes were also observed with SEM. As shown in Figure 3a, the A-KB-S electrode exhibits loose and porous structure, which is

DOI: 10.1021/am5075562
ACS Appl. Mater. Interfaces 2015, 7, 3590–3599

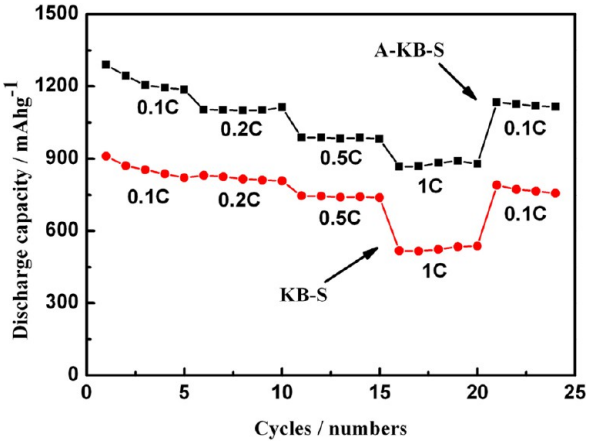

Figure 5. Rate performance of A-KB-S and KB-S composite electrodes at different discharge rates.

favorable to the mass transport and distribution. Comparatively, the KB-S electrode shows a close-grained structure (Figure 3b) due to the sulfur conglomerate outside the carbon particles, because the inner pore volume was inadequate to hold the sulfur particles. However, at higher magnification (Figure 3c,d) both electrodes exhibit similar structure agglomerated with carbon spheres. It is deduced that the water steam etching process did not destroy the morphology of the carbon particles but increased the inner pore volume and surface area, which is consistent with the result of pore structure characterization.

The basic electrochemical properties of the two C−S composites was tested via cyclic voltammetry (CV), as shown in Figure 4a, exhibiting two reduction peaks and one oxidation peak, which are attributed to the multistep reaction process of sulfur reduction reaction.[34−36] During the negative scanning, the first current peaks correspond to the reaction from sulfur to polysulfides. The 2.3 V reduction peaks correspond to the conversion of elemental sulfur to the higher-order lithium polysulfides (Li_2S_n, $n \geq 4$), and the reduction peaks at 2.1 V are associate to the further reduction of higher-order lithium polysulfides to lower-order lithium polysulfides (Li_2S_n, $n < 4$).

During the positive scanning, the oxidation peak corresponds to the reaction from the solid Li_2S and Li_2S_2 to polysulfides and sulfur.[22−24,39] Compared with KB-S, the A-KB-S shows higher reduction peak current and oxidation peak current, as well as higher onset reduction potential. Furthermore, A-KB-S composite also displays smaller ΔE (potential difference between the reduction and oxidation current peaks), indicating that the electrochemical polarization of A-KB-S is much lower than that of KB-S. This is due to that the A-KB-S composite with larger surface area and pore volume could provide more reactive sites and unobstructed Li^+ transport channels,[44] which would further facilitate the full utilization of sulfur (more capacity output, mAh g^{-1}-S).

Figure 4b compares the initial galvanostatic discharge/charge voltage profiles of the KB-S and A-KB-S composites at 0.1 C (1 C = 1675 mA g^{-1}-S) between 1.5 and 2.8 V. The discharge curves show two plateaus regions ranging from 2.3 to 2.4 V (Plateau-I) and from 2.0 to 2.1 V (Plateau-II), corresponding to the reported mechanisms for reduction and oxidation of

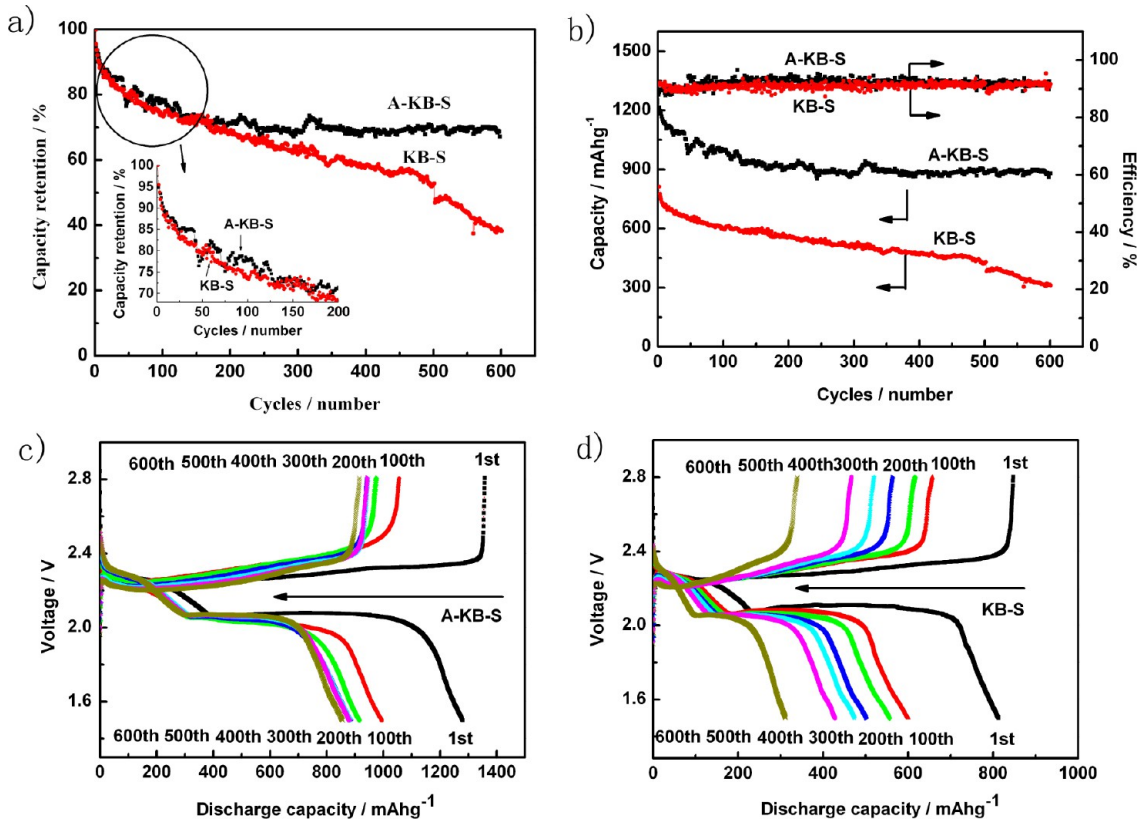

Figure 6. (a and b) Cycle performance of Li−S batteries based on the A-KB-S electrode and KB-S electrode at 0.1 C. (c and d) Galvanostatic charge/discharge voltage profiles of the A-KB-S electrode and KB-S electrode at 0.1C for the 1st, 100th, 200th, 300th, 400th, 500th, and 600th cycles.

DOI: 10.1021/am5075562
ACS Appl. Mater. Interfaces 2015, 7, 3590−3599

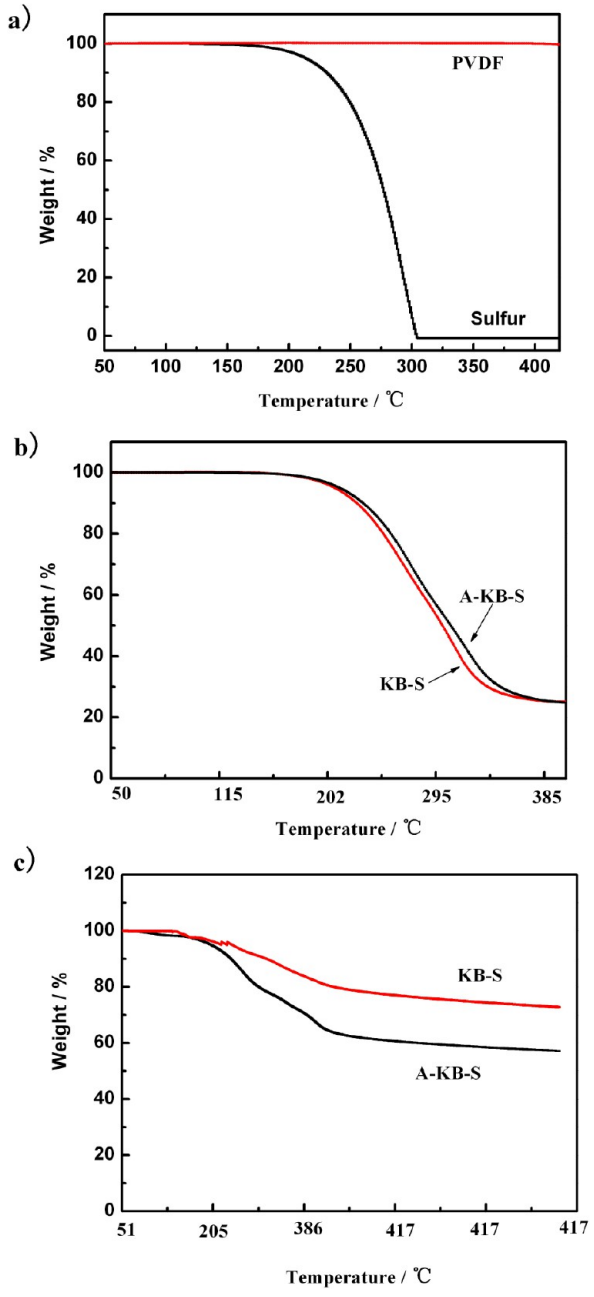

Figure 7. Thermogravimetric analysis (TGA) of the composites along with those of (a) sulfur and PVDF, (b) the sulfur content of pristine A-KB-S electrode, and the sulfur content of pristine KB-S electrode, and (c) the sulfur content of A-KB-S electrode after 300 cycles and the sulfur content of KB-S electrode after 300 cycles.

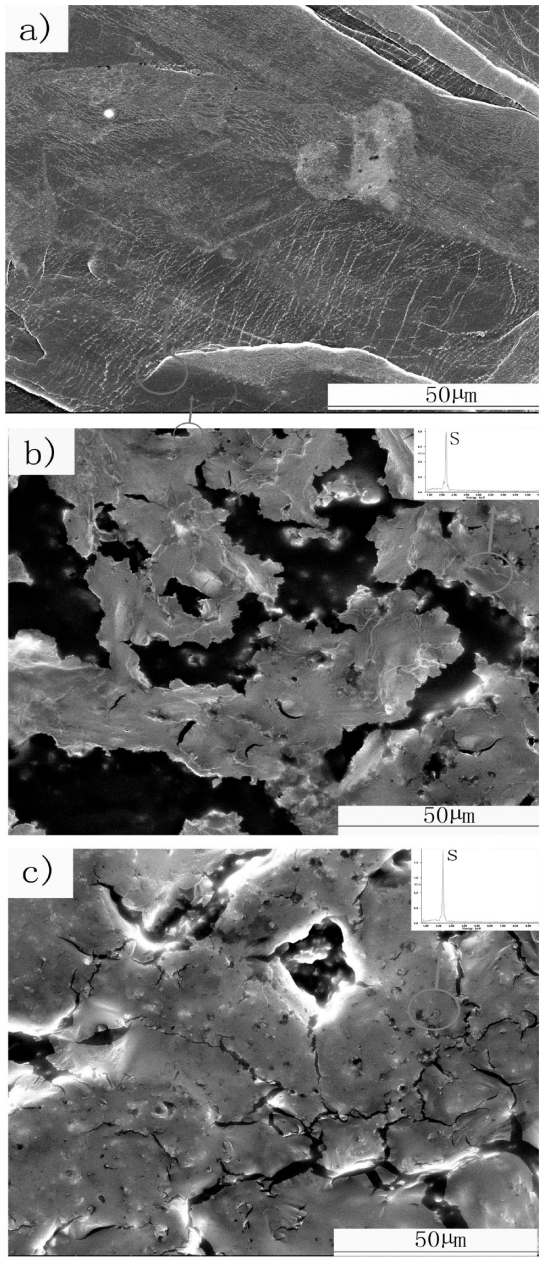

Figure 8. SEM-EDX images showing surface morphologies of (a) pristine Li-anode electrode, (b) pristine Li-anode in the battery with A-KB-S composite as cathode after 300 cycles, and (c) Li-anode in the battery with KB-S composite as cathode after 300 cycles.

elemental sulfur during discharge processes.[37] The charge curves show one plateau, which agrees well with the current peaks in CV curves. The A-KB-S composite exhibits an initial discharge capacity of about 1289 mAh g^{-1} at 0.1 C, which is about 77% of the theoretical value and much higher than that of KB-S (892 mAh g^{-1}). It also shows that the voltage gap of the A-KB-S composite between charge/discharge is smaller than that of KB-S, which is consistent with the result of CV characterization.[26]

The higher initial output capacity can be ascribed to the higher sulfur utilization in the A-KB with larger surface area and pore volume. The better electrochemical performance of A-KB-S composite at 0.1 C suggests that the lithiation/delithiation can take place more easily in its pores because more space is available for the lithium polysulfides to transport and deposit.[12,45,46]

The superior electrochemical performance of A-KB-S to that of KB-S was also analyzed on soft-pouch cells by EIS before discharge. As shown in Figure 4c, both materials exhibit typical semicircles at medium frequencies and short inclined lines in the low frequency region. The semicircle in the medium frequency region is related to the kinetic resistance of the electrochemical reaction at the electrode−electrolyte interface, which is the charge transfer resistance (R_{ct}).[38] The close contact between the conductivity material and the insulating sulfur can efficiently lower the resistance for electrons transferring across the interface between them. Hence, the A-KB-S cathode shows a smaller semicircle than that of the KB-S cathode, which

DOI: 10.1021/am5075562
ACS Appl. Mater. Interfaces 2015, 7, 3590−3599

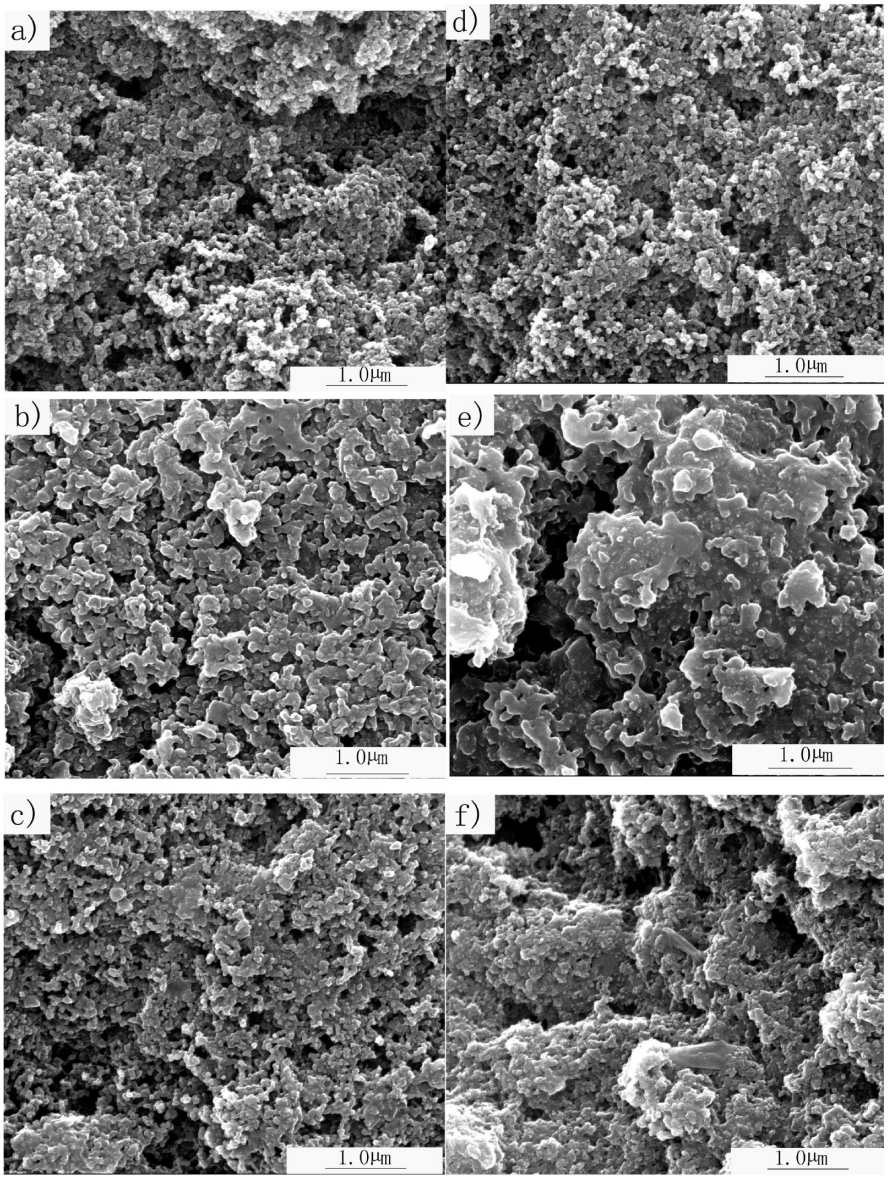

Figure 9. SEM images showing surface morphologies of 0.1 C (a) pristine A-KB-S electrode, (b) A-KB-S composite electrode, (c) A-KB-S composite electrode, (d) pristine KB-S electrode, (e) KB-S composite electrode, surface morphologies after discharging 300 cycles at 0.1 C, and (f) KB-S composite electrode, surface morphologies after charging 300 cycles at 0.1 C.

indicates better charge transfer between sulfur and carbon, originating from the uniform distribution of sulfur and easier mass transport of Li_2S_n and Li^+.[44]

The rate performance of Li/S soft package battery assembled with A-KB-S and KB-S composite cathodes was compared from 0.1 to 1 C. As shown in Figure 5, the A-KB-S composite cathode exhibits an excellent rate performance, with specific capacities of 1289, 1102, 987, and 947 mAh g^{-1} at 0.1, 0.2, 0.5, and 1 C, respectively. Furthermore, the A-KB-S composite shows higher capacities than that of KB-S at all current densities, especially at 1 C. The higher initial capacity can be ascribed to higher sulfur utilization of the A-KB-S with larger pore volume and size, which could enable better sulfur infiltration and mass/ion transport between the carbon/electrolyte interfaces.[8,33,47] As a result, the A-KB-S composite cathode also shows good capability recovery ability as the charge−discharge rate changed from 1 to 0.1 C.

Figure 6a,b show the cycle test results of Li/S soft package batteries assembled with A-KB-S and KB-S composite cathodes. For both cathodes, the capacities dropped gradually before 200 cycles at 0.1 C with the capacity retention about 70%, due to the fact that both KB and A-KB pores are in nanoscale, which suppressed the polysulfides runoff to some extent. After 600 cycles, however, the A-KB-S composite still obtained 68% capacity retention with a steady Coulombic efficiency of about 90%, while the capacity of KB-S composite drops dramatically to 38%. In addition, the discharge voltage profiles of A-KB-S composite exhibit no obvious decrease compared to KB-S composite, as shown in Figure 6c,d. In other words, the capacity retention for the A-KB-S composite decreased only 2% from 200 to 600 cycles, while the capacity retention for KB-S composite decreased 32%. This could relate to the larger pore volume in A-KB particles, which facilitates the polysulfides transport and redistribution. All in all, the increased pore volume renders the Li^+ and polysulfides easier to transfer or

DOI: 10.1021/am5075562
ACS Appl. Mater. Interfaces 2015, 7, 3590−3599

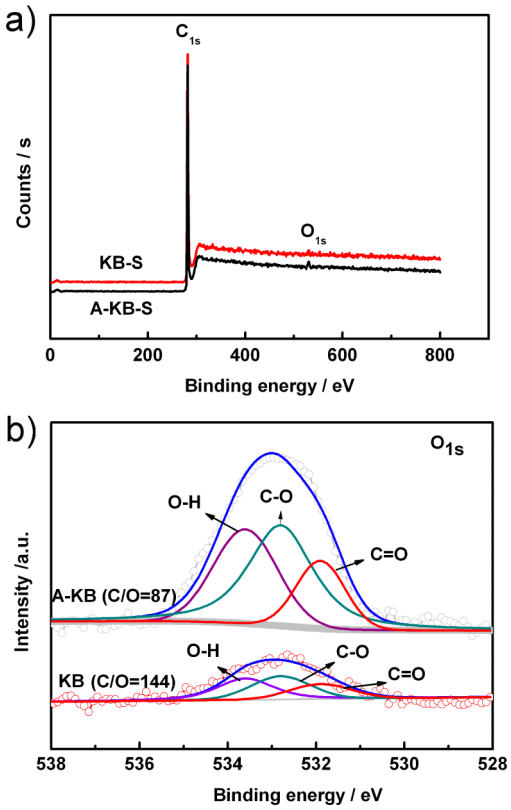

Figure 10. XPS curves of A-KB and KB carbon.

redistribution among the carbon particles, which is in favor of high capacity retention.

To better understand the relation between cycle stability and the pore structure, we carried out the sulfur content characterizations with the above two sulfur composites after 300 cycles. The tested cathodes were removed from the soft package cell at fully charged states, thoroughly washed with 1,2-dimethoxyethane (DME) to remove remaining salts, and dried in the glovebox filled with Ar. As shown in Figure 7, the initial sulfur content in the two composites is 75%. However, after 300 cycles, the sulfur content in A-KB-S is about 40%, which is much higher than that of KB-S (28%). Thus, large pore volume is beneficial to confining the polysulfides, which is in favor of capacity retention. In addition, the sulfur content in both composites after 300 cycles is far lower than the pristine ones, indicating that a large amount of polysulfides remained in electrolyte,[48] which will react with the anode. In Figure 8, the corresponding lithium anode of the two composites after 300 cycles was observed after washing with DME. In contrast to the pristine lithium, the Li-anodes are all deposited with a sulfur-containing film (Figure 8b,c) ascribed to the severe shuttle effect in both batteries.

However, the Li-anode in the battery assembled with A-KB-S composite exhibits less sulfur-containing compounds than that assembled with KB-S composite. It is speculated that the A-KB-S composite with higher porosity and pore volume can afford available channels and space for polysulfides to transport and deposit inner the carbon particles during shuttle process.

The morphology of both A-KB-S and KB-S cathodes before and after cycling 300 cycles at 0.1 C was observed via SEM. The samples were taken from the soft-pouch cells at fully charged or discharged states. As shown in Figure 9b, the A-KB-S composite electrode remains a hollow, loose structure after discharge, though the carbon spheres are covered by the slight aggregation of lithium polysulfide. However, the KB-S electrode exhibits plenty of tightly packed carbon/sulfur formed by the aggregation of lithium polysulfide, as shown in Figure 9e. It suggests that partial soluble polysulfide have broken away from the confine of the carbon pores. After charge, the A-KB-S electrode (Figure 9c) exhibits almost the same surface morphology to the initial state (Figure 9a). In contrast, there is an obvious solid layer covered on the KB-S electrode surface (Figure 9f) ascribed to the sulfur redistribution during cycling. The results demonstrate that the capacity fading of the composites electrodes is probably due to the irreversible sulfur redistribution in the carbon pores. Although partial lithium sulfides are still deposited on the outer surface of the carbon sphere as the discharge products, the sulfur is much easier to redeposit into the pores of A-KB-S composite than into those of KB-S composite due to the higher surface area and larger pore volume of A-KB-S. In other words, the sulfur distribution in pores of A-KB-S is more reversible than that of KB-S electrode, which leads to less polysulfide shuttle and less capacity fading. Overall, higher pore volume and surface area endow the C−S composite with an excellent ability to recover to the initial state, which is in favor of capacity retention during cycling.

In addition, some oxygen-containing groups are introduced into KB carbon during the water etching process, as shown in Figure 10. The intensity of oxygen-containing groups is slightly enhanced after water steam activation, with the surface O/C ratio increased by 18% (from 0.0097 to 0.0115). According to the researchers,[23,32,33] the sulfur element could be chemically bonded to the oxygen-containing groups, which could help to traps the soluble polysulfide. Thus, the increased oxygen-containing groups might also help to enhance the battery cycling stability to some extent. However, more detailed research work is needed to further clarify the functions of these oxygen-containing groups, such as −OH, −COOH, or ═O.

CONCLUSION

In summary, low-cost spherical carbon materials with large pore volume (4.0 $cm^3\ g^{-1}$) and surface area (1510 $m^2\ g^{-1}$) were prepared through a simple in situ steam etching process for use as sulfur hosts for lithium/sulfur batteries. The formation mechanism of the material morphology was investigated through the synthesis process. Carbon−sulfur composites with high sulfur content (75% S) were prepared. The relationship between the material structure and battery performance was analyzed with systematic characterizations. As a result of water steam etching, the obtained carbon material exhibits good capacity output (about 1300 mAh g^{-1}-S) and excellent capacity retention (70% after 600 cycles) at 0.1 C in Li/S battery, attributed to the reversible distribution of sulfur particles in the abundant pore volume with large surface area. It is deduced that this simple and scalable method is facile to synthesize C/S composite materials for real application and is helpful to improve the rate capability and cycle performance of Li/S batteries.

AUTHOR INFORMATION

Corresponding Authors

*Hongzhang Zhang, Tel: +86 411 8437 9669. Fax: +86 411 8466 5057. E-mail: zhanghz@dicp.ac.cn.
*Huamin Zhang, Tel: +86 411 8437 9072. Fax: +86 411 8466 5057. E-mail: zhanghm@dicp.ac.cn.

DOI: 10.1021/am5075562
ACS Appl. Mater. Interfaces 2015, 7, 3590−3599

Notes

The authors declare no competing financial interest.

■ ACKNOWLEDGMENTS

This work was supported by the National Natural Science Foundation of China (51202242).

■ REFERENCES

(1) Zhang, Y.; Zhao, Y.; Yermukhambetova, A.; Bakenov, Z.; Chen, P. Ternary Sulfur/Polyacrylonitrile/$Mg_{0.6}Ni_{0.4}O$ Composite Cathodes for High Performance Lithium/Sulfur Batteries. *J. Mater. Chem. A* **2013**, *1*, 295−301.

(2) Kolosnitsyn, V. S.; Karaseva, E. V. Lithium−Sulfur Batteries: Problems and Solutions. *Russ. J. Electrochem.* **2008**, *44*, 506−509.

(3) Hassoun, J.; Scrosati, B. Moving to a Solid-State Configuration: A Valid Approach to Making Lithium−Sulfur Batteries Viable for Practical Applications. *Adv. Mater.* **2010**, *22*, 5198−5201.

(4) Jayaprakash, N.; Shen, J.; Moganty, S. S.; Corona, A.; Archer, L. A. Porous Hollow Carbon@Sulfur Composites for High-Power Lithium−Sulfur Batteries. *Angew. Chem., Int. Ed.* **2011**, *50*, 5904−5908.

(5) Wang, J.; Chew, S. Y.; Zhao, Z. W.; Ashraf, S.; Wexler, D.; Chen, J.; Ng, S. H.; Chou, S. L.; Liu, H. K. Sulfur−Mesoporous Carbon Composites in Conjunction with a Novel Ionic Liquid Electrolyte for Lithium Rechargeable Batteries. *Carbon* **2008**, *46*, 229−235.

(6) Dutta, S.; Bhaumik, A.; Wu, K. C.-W. Hierarchically Porous Carbon Derived from Polymers and Biomass: Effect of Interconnected Pores on Energy Applications. *Energy Environ. Sci.* **2014**, *7*, 3574−3592.

(7) Zhang, B.; Lai, C.; Zhou, Z.; Gao, X. P. Preparation and Electrochemical Properties of Sulfur−Acetylene Black Composites as Cathode Materials. *Electrochim. Acta* **2009**, *54*, 3708−3713.

(8) Yuan, L.; Yuan, H.; Qiu, X.; Chen, L.; Zhu, W. Improvement of Cycle Property of Sulfur-Coated Multi-Walled Carbon Nanotubes Composite Cathode for Lithium/Sulfur Batteries. *J. Power Sources* **2009**, *189*, 1141−1146.

(9) Chen, J. J.; Jia, X.; She, Q. J.; Wang, C.; Zhang, Q.; Zheng, M. S.; Dong, Q. F. The Preparation of Nano-Sulfur/MWCNTs and Its Electrochemical Performance. *Electrochim. Acta* **2010**, *55*, 8062−8066.

(10) He, G.; Ji, X.; Nazar, L. High "C" Rate Li−S Cathodes: Sulfur Imbibed Bimodal Porous Carbons. *Energy Environ. Sci.* **2011**, *4*, 2878−2883.

(11) Liang, X.; Wen, Z.; Liu, Y.; Wu, M.; Jin, J.; Zhang, H.; Wu, X. Improved Cycling Performances of Lithium Sulfur Batteries with $LiNO_3$-Modified Electrolyte. *J. Power Sources* **2011**, *196*, 9839−9843.

(12) Zhang, B.; Qin, X.; Li, G. R.; Gao, X. P. Enhancement of Long Stability of Sulfur Cathode by Encapsulating Sulfur into Micropores of Carbon Spheres. *Energy Environ. Sci.* **2010**, *3*, 1531−1537.

(13) Li, S.; Xie, M.; Liu, J.; Wang, H.; Yan, H. Layer Structured Sulfur/Expanded Graphite Composite as Cathode for Lithium Battery. *Electrochem. Solid State Lett.* **2011**, *14*, A105−A107.

(14) Nagao, M.; Hayashi, A.; Tatsumisago, M. High-Capacity Li_2S−Nanocarbon Composite Electrode for All-Solid-State Rechargeable Lithium Batteries. *J. Mater. Chem.* **2012**, *22*, 10015−10020.

(15) Wu, F.; Qian, J.; Chen, R. J.; Lu, J.; Li, L.; Wu, H. M.; Chen, J. Z.; Zhao, T.; Ye, Y. S.; Amine, K. An Effective Approach To Protect Lithium Anode and Improve Cycle Performance for Li−S Batteries. *ACS Appl. Mater. Interfaces* **2014**, *6*, 15542−15549.

(16) Chen, R. J.; Zhao, T.; Lu, J.; Wu, F.; Li, L.; Chen, R. J.; Tan, G. Q.; Ye, Y. S.; Amine, K. Graphene-Based Three-Dimensional Hierarchical Sandwich-type Architecture for High-Performance Li/S Batteries. *Nano Lett.* **2013**, *13*, 4642−4649.

(17) Wu, F.; Chen, J. Z.; Li, L.; Zhao, T.; Liu, Z.; Chen, R. J. Polyethylene-Glycol-Doped Polypyrrole Increases the Rate Performance of the Cathode in Lithium−Sulfur Batteries. *ChemSusChem* **2013**, *6*, 1438−1444.

(18) Park, M. S.; Yu, J. S.; Kim, K. J.; Jeong, G.; Kim, J.-H.; Yim, T.; Jo, Y. N.; Hwang, U.; Kang, S.; Woo, T.; Kim, H.; Kim, Y. J. Porous Carbon Spheres as a Functional Conducting Framework for Use in Lithium−Sulfur Batteries. *RSC Adv.* **2013**, *3*, 11774−11781.

(19) Schuster, J.; He, G.; Mandlmeier, B.; Yim, T.; Lee, K. T.; Bein, T.; Nazar, L. F. Spherical Ordered Mesoporous Carbon Nanoparticles with High Porosity for Lithium−Sulfur Batteries. *Angew. Chem., Int. Ed.* **2012**, *51*, 3591−3595.

(20) Zheng, S.; Yi, F.; Li, Z.; Zhu, Y.; Xu, Y.; Luo, C.; Yang, J.; Wang, C. Copper-Stabilized Sulfur-Microporous Carbon Cathodes for Li-S Batteries. *Adv. Funct. Mater.* **2014**, *24*, 4156−4163.

(21) Zhang, Z.; Li, Z.; Hao, F.; Wang, X.; Li, Q.; Qi, Y.; Fan, R.; Yin, L. 3D Interconnected Porous Carbon Aerogels as Sulfur Immobilizers for Sulfur Impregnation for Lithium−Sulfur Batteries with High Rate Capability and Cycling Stability. *Adv. Funct. Mater.* **2014**, *24*, 2500−2509.

(22) Zhang, B.; Xiao, M.; Wang, S.; Han, D.; Song, S.; Chen, G.; Meng, Y. Novel Hierarchically Porous Carbon Materials Obtained from Natural Biopolymer as Host Matrixes for Lithium−Sulfur Battery Applications. *ACS Appl. Mater. Interfaces* **2014**, *6*, 13174−13182.

(23) Xiao, Z.; Yang, Z.; Nie, H.; Lu, Y.; Yang, K.; Huang, S. Porous Carbon Nanotubes Etched by Water Steam for High-Rate Large-Capacity Lithium−Sulfur Batteries. *J. Mater. Chem. A* **2014**, *2*, 8683−8689.

(24) Jung, D. S.; Hwang, T. H.; Lee, J. H.; Koo, H. Y.; Shakoor, R. A.; Kahraman, R.; Jo, Y. N.; Park, M. S.; Choi, J. W. Hierarchical Porous Carbon by Ultrasonic Spray Pyrolysis Yields Stable Cycling in Lithium−Sulfur Battery. *Nano Lett.* **2014**, *14*, 4418−4425.

(25) Chung, S. H.; Manthiram, A. A Natural Carbonized Leaf as Polysulfide Diffusion Inhibitor for High-Performance Lithium−Sulfur Battery Cells. *ChemSusChem* **2014**, *7*, 1655−1661.

(26) Oschatz, M.; Lee, J. T.; Kim, H.; Nickel, W.; Borchardt, L.; Cho, W. I.; Ziegler, C.; Kaskel, S.; Yushin, G. Micro- and Mesoporous Carbide-Derived Carbon Prepared by a Sacrificial Template Method in High Performance Lithium Sulfur Battery Cathodes. *J. Mater. Chem. A* **2014**, *2*, 17649−17654.

(27) Zheng, S. Y.; Chen, Y.; Xu, Y. H.; Yi, F.; Zhu, Y. J.; Liu, Y. Y.; Yang, J. H.; Wang, C. S. In Situ Formed Lithium Sulfide-Microporous Carbon Cathodes for Lithium-Ion Batteries. *ACS Nano* **2013**, *7*, 10995−11003.

(28) Jin, B.; Kim, J.; Gu, H. Electrochemical Properties of Lithium−Sulfur Batteries. *J. Power sources* **2013**, *117*, 148−152.

(29) Ma, X. Z.; Jin, B.; Xin, P. M.; Wang, H. H. Multiwalled Carbon Nanotubes-Sulfur Composites with Enhanced Electrochemical Performance for Lithium/Sulfur Batteries. *Appl. Surf. Sci.* **2014**, *307*, 346−350.

(30) Song, J. X.; Xu, T.; Gordin, M.; Zhu, P. Y.; Lv, D. P.; Jiang, Y. B.; Chen, Y. S.; Duan, Y. H.; Wang, D. H. Nitrogen-Doped Mesoporous Carbon Promoted Chemical Adsorption of Sulfur and Fabrication of High-Areal-Capacity Sulfur Cathode with Exceptional Cycling Stability for Lithium−Sulfur Batteries. *Adv. Funct. Mater.* **2014**, *24*, 1243−1250.

(31) Ma, X. Z.; Jin, B.; Wang, H. Y.; Hou, J. Z.; Zhong, X. B.; Wang, H. H.; Xin, P. M. S−TiO_2 Composite Cathode Materials for Lithium/Sulfur Batteries. *J. Electroanal. Chem.* **2015**, *736*, 127−131.

(32) Chen, X.; Xiao, Z. B.; Ning, X. T.; Liu, Z.; Yang, Z.; Zou, C.; Wang, S.; Chen, X. H.; Chen, Y.; Huang, S. H. Sulfur-Impregnated, Sandwich-Type, Hybrid Carbon Nanosheets with Hierarchical Porous Structure for High-Performance Lithium−Sulfur Batteries. *Adv. Energy Mater.* **2014**, DOI: 10.1002/aenm.201301988.

(33) Li, X.; Li, X. F.; Banis, M.; Wang, B. Q.; Lushington, A.; Cui, X. Y.; Li, R. Y.; Shamb, T. K.; Sun, X. L. Tailoring Interactions of Carbon and Sulfur in Li−S Battery Cathodes: Significant Effects of Carbon−Heteroatom Bonds. *J. Mater. Chem. A* **2014**, *2*, 12866−12872.

(34) Qiu, L.; Zhang, S.; Zhang, L.; Sun, M.; Wang, W. Preparation and Enhanced Electrochemical Properties of Nano-Sulfur/Poly-(pyrrole-co-aniline) Cathode Material for Lithium/Sulfur Batteries. *Electrochim. Acta* **2010**, *55*, 4632−4636.

(35) Peled, E.; Gorenshtein, A.; Segal, M.; Sternberg, Y. Rechargeable Lithium Sulfur Battery. *J. Power Sources* **1989**, *26*, 269−271.

(36) Choi, Y. J.; Chung, Y. D.; Baek, C. Y.; Kim, K. W.; Ahn, H. J.; Ahn, J. H. Effects of Carbon Coating on the Electrochemical

DOI: 10.1021/am5075562
ACS Appl. Mater. Interfaces 2015, 7, 3590−3599

Properties of Sulfur Cathode for Lithium/Sulfur Cell. *J. Power Sources* **2008**, *184*, 548−552.
(37) Han, S. C.; Song, M. S.; Lee, H.; Kim, H. S.; Ahn, H. J.; Lee, J. Y. Effect of Multiwalled Carbon Nanotubes on Electrochemical Properties of Lithium/Sulfur Rechargeable Batteries. *J. Electrochem. Soc.* **2003**, *150*, A889−A893.
(38) He, M.; Yuan, L. X.; Zhang, W. X.; Hu, X. L.; Huang, Y. H. Enhanced Cyclability for Sulfur Cathode Achieved by a Water-Soluble Binder. *J. Phys. Chem. C* **2011**, *115*, 15703−15709.
(39) Sohn, H.; Gordin, M. L.; Xu, T.; Chen, S.; Lv, D.; Song, J.; Manivannan, A.; Wang, D. Porous Spherical Carbon/Sulfur Nanocomposites by Aerosol-Assisted Synthesis: The Effect of Pore Structure and Morphology on Their Electrochemical Performance as Lithium/Sulfur Battery Cathodes. *ACS Appl. Mater. Interfaces* **2014**, *6*, 7596−606.
(40) Wang, M.; Wang, W.; Wang, A.; Yuan, K.; Miao, L.; Zhang, X.; Huang, Y.; Yu, Z.; Qiu, J. A Multi-Core-Shell Structured Composite Cathode Material with a Conductive Polymer Network for Li−S Batteries. *Chem. Commun.* **2013**, *49*, 10263−10265.
(41) Wang, M.; Zhang, H.; Zhang, Y.; Li, J.; Zhang, F.; Hu, W. A Modified Hierarchical Porous Carbon for Lithium/Sulfur Batteries with Improved Capacity and Cycling Stability. *J. Solid State Electrochem.* **2013**, *17*, 2243−2250.
(42) Li, X.; Cao, Y.; Qi, W.; Saraf, L. V.; Xiao, J.; Nie, Z.; Mietek, J.; Zhang, J. G.; Schwenzer, B.; Liu, J. Optimization of Mesoporous Carbon Structures for Lithium−Sulfur Battery Applications. *J. Mater. Chem.* **2011**, *21*, 16603−16610.
(43) González, P. G.; Pliego-Cuervo, Y. B. Physicochemical and Microtextural Characterization of Activated Carbons Produced from Water Steam Activation of Three Bamboo Species. *J. Anal. Appl. Pyrolysis* **2013**, *99*, 32−39.
(44) Xu, G.; Ding, B.; Nie, P.; Shen, L.; Dou, H.; Zhang, X. Hierarchically Porous Carbon Encapsulating Sulfur as a Superior Cathode Material for High Performance Lithium−Sulfur Batteries. *ACS Appl. Mater. Interfaces* **2014**, *6*, 194−199.
(45) Thieme, S.; Brückner, J.; Bauer, I.; Oschatz, M.; Borchardt, L.; Althues, H.; Kaskel, S. High Capacity Micro-Mesoporous Carbon−Sulfur Nanocomposite Cathodes with Enhanced Cycling Stability Prepared by a Solvent-Free Procedure. *J. Mater. Chem. A* **2013**, *1*, 9225−9234.
(46) Zheng, J.; Lv, D.; Gu, M.; Wang, C.; Zhang, J. G.; Liu, J.; Xiao, J. How to Obtain Reproducible Results for Lithium Sulfur Batteries? *J. Electrochem. Soc.* **2013**, *160*, A2288−A2292.
(47) Park, J. W.; Ueno, K.; Tachikawa, N.; Dokko, K.; Watanabe, M. Ionic Liquid Electrolytes for Lithium−Sulfur Batteries. *J. Phys. Chem. C* **2013**, *117*, 20531−20541.
(48) Xiong, S.; Xie, K.; Diao, Y.; Hong, X. Oxidation Process of Polysulfides in Charge Process for Lithium−Sulfur Batteries. *Ionics* **2012**, *18*, 867−872.

DOI: 10.1021/am5075562
ACS Appl. Mater. Interfaces 2015, 7, 3590−3599